ACS Macro Letters

Letter

pubs.acs.org/macroletters

Atomic Force Microscopy Observation of Polylactide Stereocomplex Edge-On Crystals in Thin Films: Effects of Molecular Weight on Lamellar Curvature

Hironori Marubayashi, Toshihiro Nobuoka, Shinichiro Iwamoto, Akio Takemura, and Tadahisa Iwata*

Science of Polymeric Materials, Department of Biomaterial Sciences, Graduate School of Agricultural and Life Sciences, The University of Tokyo, 1-1-1 Yayoi, Bunkyo-ku, Tokyo 113-8657, Japan

ABSTRACT: The shapes of the edge-on lamellar crystals of equiweight poly(L-lactide) (PLLA)/poly(D-lactide) (PDLA) stereocomplexes with various combinations of molecular weights were investigated by using atomic force microscopy. In the cases of the PLLA/PDLA blends with equivalent molecular weights, the straight-shaped edge-on lamellae were observed. On the other hand, the curved edge-on crystals were able to be seen for the PLLA/PDLA stereocomplexes with nonequivalent molecular weights. It was revealed that the direction of lamellar curvature in the polylactide (PLA) stereocomplexes with nonequivalent molecular weights is the same as that of PLA having lower molecular weight. In addition to the PLLA/PDLA blending ratio, *the incidence of chain folding*, which is strongly influenced by molecular weight, was considered to have a crucial effect on the lamellar curvature in the edge-on crystals of PLA stereocomplexes.

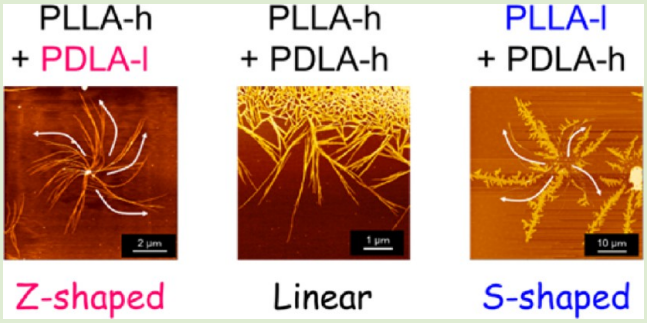

Polylactide (PLA) is one of the biobased polymers expected to be alternatives to the petroleum-based polymers.[1] PLA has optically active enantiomers due to the chirality of the monomer: poly(L-lactide) (PLLA) and poly(D-lactide) (PDLA).

It is well-known that PLLA forms several types of crystal structures (crystal polymorphism) depending on the surrounding conditions: α-,[2,3] α' (δ)-,[4,5] α''-,[6] β-,[7] and γ-[8]forms. Furthermore, PLLA forms the cocrystals with the specific low-molecular-weight compounds in the specific conditions: CO_2 complex[6] and solvent complex (ε-form).[9] Roughly speaking, PLLA chains take the 10/7 (left-handed 10/3) helical conformation in the α, α', CO_2 complex, and solvent complexes and the 3/2 (left-handed 3/1) helical conformation in the β- and γ-forms. For the PLLA crystals with 10/7 helices (α, α', and ε), it was reported that PLLA chains are distorted from the ideal 10/7 helix.[3,5,9] The α-form, which is considered to be the most stable phase of PLLA, possesses the orthorhombic unit cell with a = 1.068 nm, b = 0.617 nm, and c (fiber axis) = 2.886 nm (25 °C).[5]

In 1987, Ikada et al. discovered that PLLA and PDLA crystallize into a 1/1 stereocomplex, which exhibits a 50 °C higher melting point compared to the enantiomeric components.[10] In the stereocomplexation, PLLA 3/2 and PDLA 3/1 helices are packed side by side in the unit cell (triclinic[11,12] or trigonal;[13,14] the latter would be preferred in terms of the symmetry). The lattice constants of the trigonal cell of the PLA stereocomplex are as follows: $a = b$ = 1.498 nm, c (fiber axis) = 0.870 nm, $\alpha = \beta = 90°$, and $\gamma = 120°$.[13] The highly unusual triangular morphology is observed in single crystals of the PLLA/PDLA stereocomplex.[12,13]

Recently, the crystalline morphologies of PLA in thin films have been investigated by means of atomic force microscopy (AFM). Kikkawa et al. proposed that the different thermal behavior of each sector in PLLA lamellar crystals (100 and 110) can be explained in terms of the chain folding, crystal growth direction, and molecular chain packing.[15] They also reported that the edge-on PLLA lamellar crystals, which have nucleated and elongated at the initial stage of crystallization, show the S-shaped morphology and change their orientation from edge-on manner to flat-on one.[16] Maillard and Prud'homme revealed that the PLLA edge-on lamellae are S-shaped and the PDLA Z-shaped in ultrathin films (15 nm) using AFM.[17,18] Furthermore, it was proposed that the direction of curvature of the lamellae can be linked with the sense of twisting of the PLA lamellae in banded spherulites on a micrometer scale, and the temperature dependence of the radius of curvature can be correlated to the distance between the extinction rings. They also showed that the equimolar PLA stereocomplex exhibits a hexagonal crystal shape that becomes triangular for the nonequimolar mixtures (dendritic flat-on crystals).[19] In addition, the primary and secondary branches of the triangular dendritic crystals, obtained at thicknesses of 20 nm, exhibited a circular crystallization mode (clockwise when PDLA is in excess and counterclockwise when PLLA is in excess). In contrast, in the

Received: January 9, 2013
Accepted: April 8, 2013
Published: April 11, 2013

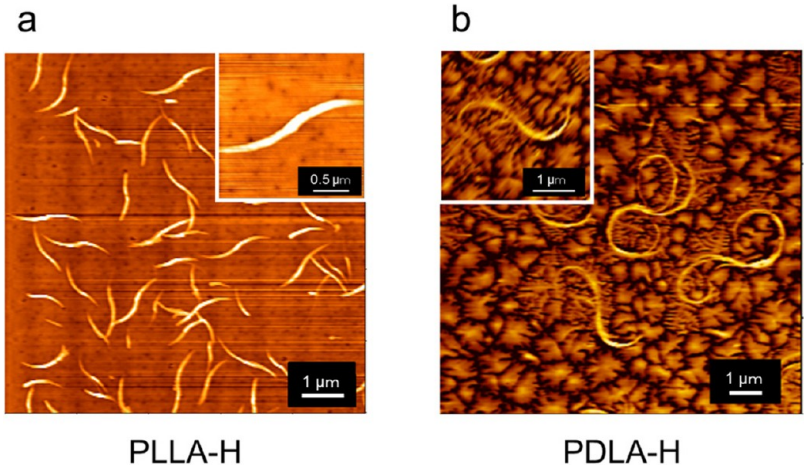

Figure 1. AFM height images of PLA thin films: (a) PLLA-H melt-crystallized at 120 °C for 30 min and (b) PDLA-H melt-crystallized at 120 °C for 60 min. Zoom-in images are also shown in the upper right corner (a) and the upper left corner (b).

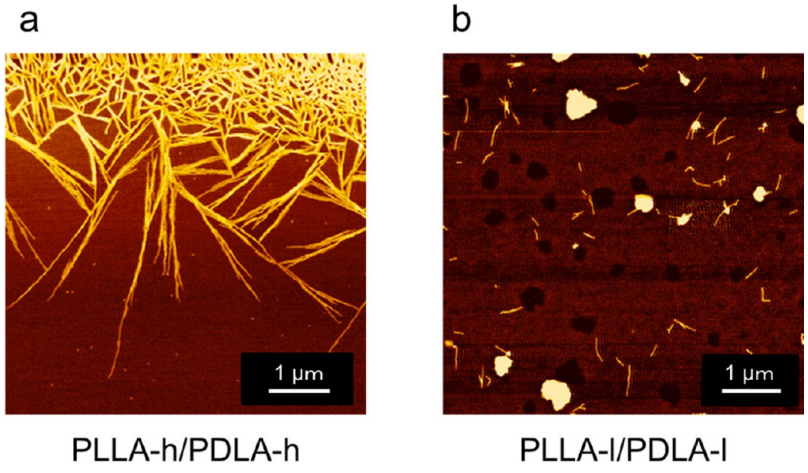

Figure 2. AFM height images of PLLA/PDLA thin films with equivalent molecular weights: (a) PLLA-h/PDLA-h melt-crystallized at 180 °C for 1 h and (b) PLLA-l/PDLA-l melt-crystallized at 170 °C for 24 h.

hexagonal dendritic crystal (equimolar PLA stereocomplex), the primary and secondary branches grew linearly.

The PLLA/PDLA stereocomplexation is known to strongly depend on the blend ratios of polyenantiomers, the molecular weights of polyenantiomers, the annealing time, and the annealing temperature.[20] Furthermore, the different stereocomplexation behavior is seen between dry and wet processes.[21] As far as we know, there have been no reports on the effect of molecular weight on the lamellar curvature of the PLA stereocomplex. In this paper, we investigated the shapes of the edge-on crystals of equiweight PLLA/PDLA stereocomplexes in various combinations of molecular weights using AFM. We propose the idea that *the incidence of chain folding*, which is strongly affected by molecular weight, has a great effect on the lamellar curvature in the edge-on crystal of the PLA stereocomplex.

Figure 1 shows the edge-on crystals of PLLA-H and PDLA-H in thin films (homocrystals). The S-shaped PLLA edge-on crystals with a length of 1−2 μm were observed, while the Z-shaped PDLA lamellae with several micrometers length were confirmed, as previously reported.[16−18] Such a definite relationship between the direction of lamellar curvature and the chain chirality can be explained by two reasons:[18] one is the difference of the chain-folding direction on the two sides of the lamella, and the other is the exit angle with a specific value of the chain from the lamella. The lamellar curvature and twist are considered to be driven by the unbalanced surface stresses on the lamellar crystal.[17−19,22−27] The Keith−Padden model shows that the chain tilt relative to the lamellar basal plane is responsible for differential aggregation of the chain folds on the lamellar surfaces, which brings about the unbalanced surface stresses and results in curving and twisting of crystalline lamellae.[22,27]

Figure 2 exhibits the edge-on lamellae of PLLA/PDLA stereocomplexes with equivalent molecular weights. Crystallization temperatures were set to 170−180 °C, at which only the stereocomplexation occurs (melting of homocrystals of PLLA and PDLA). For both PLLA-h/PDLA-h and PLLA-l/PDLA-l, the edge-on crystals were observed, although there is a difference in the length of the edge-on lamella. In the case of the PLLA-l/PDLA-l blend (Figure 2b), a small number of flat-on crystals were also seen. As can be seen, the edge-on crystals grew linearly and showed no curvature for both PLLA-h/PDLA-h and PLLA-l/PDLA-l. This result is in good agreement with the case of dendritic flat-on crystals of the equimolar PLA stereocomplex reported by Maillard and Prud'homme.[19] Because of the symmetry of the trigonal unit cell, in which three PLLA chains and three PDLA ones are contained,[13] the

dx.doi.org/10.1021/mz400014s | *ACS Macro Lett.* 2013, 2, 355−360

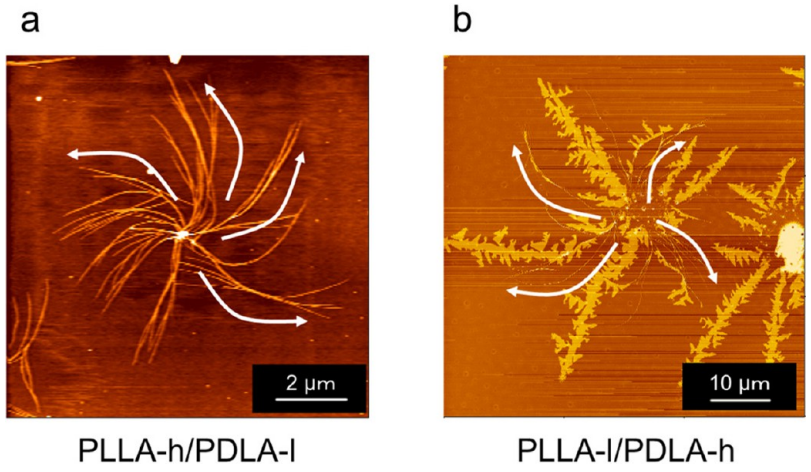

Figure 3. AFM height images of PLLA/PDLA thin films with nonequivalent molecular weights: (a) PLLA-h/PDLA-l melt-crystallized at 180 °C for 1 h and (b) PLLA-l/PDLA-h melt-crystallized at 180 °C for 24 h.

chains exit from the crystal with a specific angle, and this angle is inverted from PLLA to PDLA.[19] The top surface of the lamella is constituted of an equal number of PLLA and PDLA chains, so that the surface stresses would cancel each other out, resulting in the formation of linear edge-on crystals.

Figure 3 displays the edge-on lamellae of PLLA/PDLA stereocomplexes with significantly different molecular weights (PLLA-h/PDLA-l and PLLA-l/PDLA-h). For both cases, the radial crystal growth from a core can be seen. The length from the core to the crystal growth front was several micrometers for PLLA-h/PDLA-l (Figure 3a) and longer than 10 μm for PLLA-l/PDLA-h (Figure 3b). For the PLLA-l/PDLA-h blend (Figure 3b), dendritic crystals as well as edge-on crystals were observed. Interestingly, the edge-on crystals of the PLLA-h/PDLA-l stereocomplex curved in the left direction (Z-shape: Figure 3a), whereas those of the PLLA-l/PDLA-h stereocomplex showed the curvature in the right direction (S-shape: Figure 3b). Thus, in the PLA stereocomplexes with nonequivalent molecular weights, it was found that the edge-on crystals show the lamellar curvature, and the direction of curvature is the same as that of PLA having lower molecular weight.

Why does the edge-on lamella of equiweight PLA stereocomplexes show the curvature by following the polyenantiomer with *lower* molecular weight? In answer to this question, we propose here that *the incidence of chain folding* has a key role in determining the lamellar curvature of equiweight PLLA/PDLA stereocomplexes with significantly different molecular weights. With decreasing molecular weight, the chain folding would occur with a lower incidence. When the chain length reduces sufficiently, polymer chains would no longer fold, i.e., the formation of crystals composed of the extended chains. Kawai et al. mentioned the difficulty in the occurrence of the extended chain crystals, which may be attributed to the reductions in the entropy of the system on the extension of the coiled chains and the gathering of the extended chains and would be highly dependent upon molecular weight.[28] The ratio that polymer chains exit from the lamella surface without folding (R_{exit}) will be approximated by the following equation

$$R_{exit} = \frac{2}{(M/M_{min}) \times 2} \times 100 \quad (1)$$

where M is the molecular weight of polymer and M_{min} is the molecular weight corresponding to the lamellar thickness containing the length of folded segments. The numerator (2) means the number of chain ends per molecule, and the denominator represents the number of chains passing through the interior−surface boundary of the lamella. The possibility that two separate chains pair their ends within the crystal makes the situation rather complicated and hence is not considered here. In addition, the folding manner was assumed to be sharp folds, not loose loops. Assuming that the lamellar thickness is independent of M, it follows that M_{min} shows a constant value. In this case, R_{exit} can be represented by only M ($R_{exit} \propto M^{-1}$). The lamellar thickness containing the length of folded segments, which is needed to calculate M_{min}, was obtained from the flat-on lamellar crystals of various PLA stereocomplexes because the accuracy in the height direction is superior to that in the width direction for AFM observation. As a result, the averaged lamellar thickness (l) was 8.7 nm. The fiber period is 0.87 nm, which is the same as the c-axis length because of the *ab* plane perpendicular to c (chain axis direction) for the PLLA/PDLA stereocomplex.[13,14] The molecular weight per fiber period (three residues) M_{fp} is 216. Therefore, $M_{min} = l/c \times M_{fp} = 2160$. Figure 4 shows the molecular weight (M) dependence of R_{exit}. As can be seen, R_{exit} increases with decreasing molecular weight, and when the molecular weight becomes smaller than 1×10^4, there is a drastic increase in R_{exit} with decreasing molecular weight. When M_w was used as M, R_{exit}'s for our PLA samples were calculated as follows: 2% for PLLA-h, 48% for PLLA-l, 1% for PDLA-h, and 58% for PDLA-l.

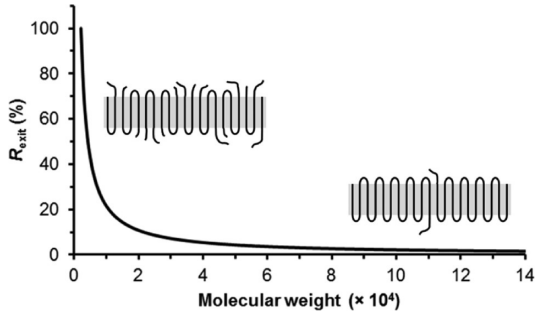

Figure 4. Ratio that PLA chains exit from the lamella without folding (R_{exit}) as a function of molecular weight. Schematic illustrations representing a difference in the incidence of chain folding are also shown.

dx.doi.org/10.1021/mz400014s | *ACS Macro Lett.* 2013, 2, 355−360

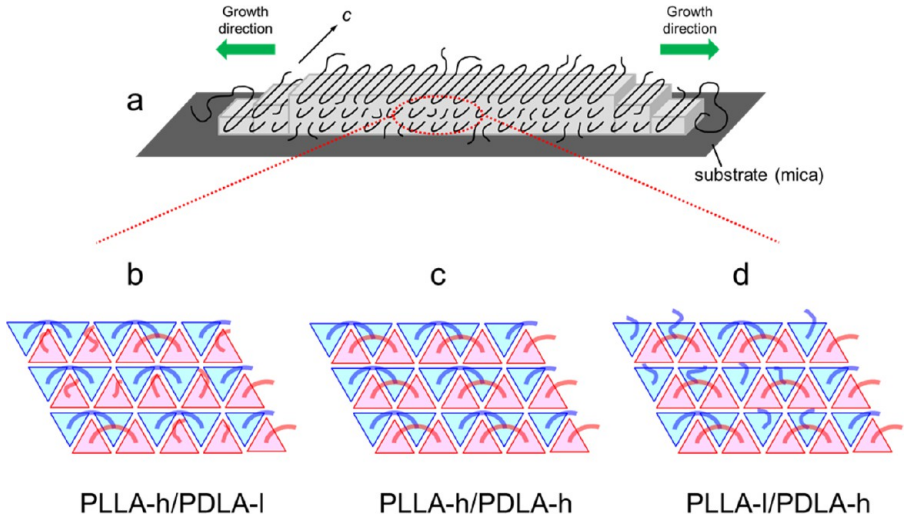

Figure 5. Top (a): schematic representation of the edge-on crystal of the PLLA/PDLA stereocomplex, in which the region enclosed by a red dotted line is focused below. Bottom (b, c, d): schematic illustration showing a difference in the incidence of chain folding for PLLA and PDLA chains in the edge-on stereocomplex crystals with various combinations of molecular weights, in which blue and red triangles represent PLLA and PDLA chains, respectively (axial view): (b) PLLA-h/PDLA-l, (c) PLLA-h/PDLA-h, and (d) PLLA-l/PDLA-h.

Thus, the incidence of chain folding can be controlled by changing the molecular weight of PLA.

For the PLA stereocomplexes with equivalent molecular weights (PLLA-h/PDLA-h and PLLA-l/PDLA-l), the edge-on lamellae grew linearly (Figure 2). On the other hand, in the cases of the PLLA/PDLA stereocomplexes with nonequivalent molecular weights (i.e., PLLA-h/PDLA-l and PLLA-l/PDLA-h), the curvature of the edge-on lamella was observed (Figure 3). In the latter case, there should be a significant difference in the incidence of chain folding between PLLA and PDLA, as expected from eq 1 (Figure 4). As mentioned above, the chain folding naturally induces a stress on the lamellar surface and leads to the lamellar curvature.[17−19,22−27] Here, it should be reasonable to consider that the stress induced by the folded segments is different from that given by the segments which exit from the lamella without folding (unfolded segments). If so, there would be a substantial difference in the magnitude of surface stress between the PLA enantiomer with higher molecular weight (lower R_{exit}) and that with lower molecular weight (higher R_{exit}). As a result, there should remain the unbalanced surface stresses, resulting in the formation of curved edge-on crystals.

Figure 5 is a schematic illustration of a difference in the incidence of chain folding for PLLA and PDLA chains in the edge-on stereocomplex lamellae having various combinations of molecular weights. For both PLLA-h/PDLA-h (Figure 5c) and PLLA-l/PDLA-l (not shown), the magnitude of the overall stress on the lamellar surface can be approximated to zero, leading to the formation of linear edge-on lamellae (Figure 2). In the cases of PLLA-h/PDLA-l (Figure 5b) and PLLA-l/PDLA-h (Figure 5d), the remaining surface stresses would possess the opposite direction, resulting in the opposite curving direction of lamellar crystals, as shown in Figure 3. Since the curving direction of the edge-on lamella followed the polyenantiomer with lower molecular weight (higher R_{exit}), we propose here that the surface stress induced by the unfolded segments is higher than that derived from the folded segments.

Taking into account polydispersity (M_w/M_n) of our PLA samples, there would be distribution in R_{exit}. Although PLLA-l has relatively high polydispersity (2.74), M_n and M_w themselves are much lower than those of PLLA-h and PDLA-h (double-digit difference). Therefore, the above-mentioned discussion on R_{exit} would be valid. In addition, relatively low T_g of PDLA-l (22 °C) implies that its molecular weight is below the entanglement molecular weight (M_e). M_e of PLA has been reported to be 8700−10 500 g/mol.[29,30] Although M_w of PLLA-l is also below the reported M_e values, relatively high polydispersity (2.74) as well as slightly higher molecular weight should be responsible for much higher T_g (40 °C) compared to PDLA-l (22 °C). Here, when molecular weight reduces to around the reported M_e values, R_{exit} shows a drastic increase (Figure 4), implying the correlation between M_e and the chain folding.

In summary, AFM observation revealed that molecular weight has a great effect on the curvature of the edge-on crystals of equiweight PLLA/PDLA stereocomplexes. The correlation between the curving direction of the edge-on lamella and molecular weight was reasonably understood in terms of the incidence of chain folding. The insight into the molecular weight dependence of the lamellar curvature of equiweight PLA stereocomplexes is expected to be of great help for better understanding of the lamellar twisting and the spherulitic morphology (e.g., banded morphology) in the stereocomplexes with various combinations of molecular weights.

■ EXPERIMENTAL SECTION

Samples. PLA (PLLA and PDLA) samples with different molecular weights were used in this study. Weight-average molecular weight (M_w), polydispersity (M_w/M_n), specific optical rotation ($[\alpha]^{23}_D$), and thermal properties [glass transition temperature (T_g), crystallization temperature (T_c), and melting temperature (T_m)] of PLLA and PDLA used are summarized in Table 1. High-molecular-weight PLLA and PDLA, which were named "PLLA-H" and "PDLA-H", respectively, were used only for studies on homocrystals. PLLA-H was supplied from Shimadzu Corp., and PDLA-H was provided by Dr. Lee from Pukyong National University. As samples for stereocomplexes, two kinds of PLLA and two kinds of PDLA with different molecular weights were chosen. PLLA having higher molecular weight was named "PLLA-h", and that with lower molecular weight was referred to as "PLLA-l". "PDLA-h" and "PDLA-l" were defined in a similar way. PLLA-h was purchased from Polysciences, Inc.; PDLA-h

dx.doi.org/10.1021/mz400014s | ACS Macro Lett. 2013, 2, 355−360

Table 1. Molecular Weight, Specific Optical Rotation, and Thermal Properties of PLLA and PDLA Used in This Study

name	M_w[c]	M_w/M_n[c]	$[\alpha]^{23}_D$[d]	T_g[e] (°C)	T_c[e] (°C)	T_m[e] (°C)
PLLA-H[a]	2.77×10^5	1.44	−152	61	122	169
PLLA-h[b]	1.22×10^5	1.51	−153	49	101	168
PLLA-l[b]	4.49×10^3	2.74	−144	40	92	128
PDLA-H[a]	6.93×10^4	1.41	143	56	103	168
PDLA-h[b]	1.67×10^5	1.63	153	59	122	172
PDLA-l[b]	3.70×10^3	1.16	125	22	72	116

[a]Used only for homocrystals. [b]Used only for stereocomplexes. [c]Measured by gel permeation chromatography with $CHCl_3$ as a diluent and polystyrene as a standard. [d]The specific optical rotation (degree dm^{-1} g^{-1} mL) measured by a polarimeter (c = 1.0 g/dL, 23 °C, $CHCl_3$). [e]Measured by differential scanning calorimetry (second run, 20 °C/min).

was supplied from Teijin, Ltd.; and PDLA-l was provided by Dr. Lee from Pukyong National University. PLLA-l was synthesized by ring-opening polymerization of L-lactide at 60 °C for the desired period with stannous 2-ethyl hexanoate as a catalyst.

Preparation of PLA Homocrystal Thin Films. PLLA-H thin films were prepared by spin-coating of 20 μL of chloroform solution of PLLA-H with a concentration of 0.1 wt % on a mica substrate at a rotation speed of 2000 rpm for 1 min. Preparation of PDLA-H thin films was conducted in a similar way. To obtain PLA homocrystals, PLLA-H and PDLA-H thin films were annealed at 120 °C for 30−60 min after melting at 220 °C.

Preparation of PLA Stereocomplex Thin Films. First, PLLA thin films were prepared by spin-coating of 20 μL of chloroform solution of PLLA (PLLA-h or PLLA-l) with a concentration of 0.25 wt % on a mica substrate at a rotation speed of 2000 rpm for 1 min. Second, chloroform solution of PDLA-h or PDLA-l (0.25 wt %, 20 μL) was spin-coated on the PLLA thin film on a mica substrate. As a result, a total of four types of PLLA/PDLA thin films were prepared (PLLA-h/PDLA-h, PLLA-h/PDLA-l, PLLA-l/PDLA-h, and PLLA-l/PDLA-l). For stereocomplexation, the obtained thin films were crystallized at 170−180 °C for 1−24 h after melting at 240 °C.

Atomic Force Microscopy. The surface morphologies of PLA thin films were observed by using a scanning probe system comprising SPA-300 and SN-3800 (SII nanotechnology Inc.) units and a cantilever (SN-AF-01, SII nanotechnology Inc.) in a dynamic force microscope (DFM) mode.

AUTHOR INFORMATION

Corresponding Author

*Tel. +81-3-5841-5266. Fax: +81-3-5841-1304. E-mail: atiwata@mail.ecc.u-tokyo.ac.jp.

Notes

The authors declare no competing financial interest.

ACKNOWLEDGMENTS

We thank Teijin, Ltd. (Japan), Shimadzu Corp. (Japan), and Dr. W.-K. Lee (Pukyong National University, Korea) for supplying PLA samples. We thank Dr. H. Abe (RIKEN, Japan) for letting H.M. use a polarimeter. This work was supported by the Grant-in-Aid for Scientific Research (A) (no. 22245026) from the Japan Society for the Promotion of Science.

REFERENCES

(1) (a) *Bio-Based Polymers: Recent Progress*; Im, S. S., Kim, Y. H., Yoon, J. S., Chin, I.-J., Eds.; Macromolecular Symposia; Wiley-VCH: Weinheim, Germany, 2005. (b) *Biodegradable Polymers and Plastics*; Chiellini, E., Solaro, R., Eds.; Kluwer Academic/Plenum Publishers: New York, 2003. (c) *Poly(lactic acid): Synthesis, Structures, Properties, Processing, and Applications*; Auras, R., Lim, L.-T., Selke, S. E. M., Tsuji, H., Eds.; Wiley Series on Polymer Engineering and Technology; Wiley: Hoboken, NJ, 2010. (d) Gandini, A. *Macromolecules* **2008**, *41*, 9491−9504. (e) Coates, G. W.; Hillmyer, M. A. *Macromolecules* **2009**, *42*, 7987−7989.

(2) (a) Santis, P. D.; Kovacs, A. J. *Biopolymers* **1968**, *6*, 299−306. (b) Hoogsteen, W.; Postema, A. R.; Pennings, A. J.; ten Brinke, G.; Zugenmaier, P. *Macromolecules* **1990**, *23*, 634−642. (c) Aleman, C.; Lotz, B.; Puiggali, J. *Macromolecules* **2000**, *34*, 4795−4801.

(3) (a) Sasaki, S.; Asakura, T. *Macromolecules* **2003**, *36*, 8385−8390. (b) Wasanasuk, K.; Tashiro, K.; Hanesaka, M.; Ohhara, T.; Kurihara, K.; Kuroki, R.; Tamada, T.; Ozeki, T.; Kanamoto, T. *Macromolecules* **2011**, *44*, 6441−6452.

(4) (a) Zhang, J.; Duan, Y.; Sato, H.; Tsuji, H.; Noda, I.; Yan, S.; Ozaki, Y. *Macromolecules* **2005**, *38*, 8012−8021. (b) Zhang, J.; Tashiro, K.; Domb, A. J.; Tsuji, H. *Macromol. Symp.* **2006**, *242*, 274−278. (c) Zhang, J.; Tashiro, K.; Tsuji, H.; Domb, A. J. *Macromolecules* **2008**, *41*, 1352−1357. (d) Cho, T. Y.; Strobl, G. *Polymer* **2006**, *47*, 1036−1043. (e) Kawai, T.; Rahman, N.; Matsuba, G.; Nishida, K.; Kanaya, T.; Nakano, M.; Okamoto, H.; Kawada, J.; Usuki, A.; Honma, N.; Nakajima, K.; Matsuda, M. *Macromolecules* **2007**, *40*, 9463−9469. (f) Pan, P.; Kai, W.; Zhu, B.; Dong, T.; Inoue, Y. *Macromolecules* **2007**, *40*, 6898−6905.

(5) (a) Wasanasuk, K.; Tashiro, K. *Polymer* **2011**, *52*, 6097−6109. (b) Wasanasuk, K.; Tashiro, K. *Macromolecules* **2011**, *44*, 9650−9660.

(6) (a) Marubayashi, H.; Akaishi, S.; Akasaka, S.; Asai, S.; Sumita, M. *Macromolecules* **2008**, *41*, 9192−9203. (b) Marubayashi, H.; Asai, S.; Sumita, M. *Polymer* **2012**, *53*, 4262−4271.

(7) (a) Eling, B.; Gogolewski, S.; Pennings, A. J. *Polymer* **1982**, *23*, 1587−1593. (b) Puiggali, J.; Ikada, Y.; Tsuji, H.; Cartier, L.; Okihara, T.; Lotz, B. *Polymer* **2000**, *41*, 8921−8930. (c) Sawai, D.; Takahashi, K.; Imamura, T.; Nakamura, K.; Kanamoto, T.; Hyon, S.-H. *J. Polym. Sci., Part B: Polym. Phys.* **2002**, *40*, 95−104. (d) Sawai, D.; Takahashi, K.; Sasashige, A.; Kanamoto, T.; Hyon, S.-H. *Macromolecules* **2003**, *36*, 3601−3605.

(8) Cartier, L.; Okihara, T.; Ikada, Y.; Tsuji, H.; Puiggali, J.; Lotz, B. *Polymer* **2000**, *41*, 8909−8919.

(9) (a) Marubayashi, H.; Asai, S.; Sumita, M. *Macromolecules* **2012**, *45*, 1384−1397. (b) Marubayashi, H.; Asai, S.; Sumita, M. *J. Phys. Chem. B* **2013**, *117*, 385−397.

(10) Ikada, Y.; Jamshidi, K.; Tsuji, H.; Hyon, S.-H. *Macromolecules* **1987**, *20*, 904−906.

(11) Okihara, T.; Tsuji, M.; Kawaguchi, A.; Katayama, K.-I.; Tsuji, H.; Hyon, S.-H.; Ikada, Y. *J. Macromol. Sci., Part B: Phys.* **1991**, *B30*, 119−140.

(12) Brizzolara, D.; Cantow, H.-J.; Diederichs, K.; Keller, E.; Domb, A. J. *Macromolecules* **1996**, *29*, 191−197.

(13) Cartier, L.; Okihara, T.; Lotz, B. *Macromolecules* **1997**, *30*, 6313−6322.

(14) Sawai, D.; Tsugane, Y.; Tamada, M.; Kanamoto, T.; Sungil, M.; Hyon, S.-H. *J. Polym. Sci., Part B: Polym. Phys.* **2007**, *45*, 2632−2639.

(15) Kikkawa, Y.; Abe, H.; Iwata, T.; Inoue, Y.; Doi, Y. *Biomacromolecules* **2002**, *3*, 350−356.

(16) Kikkawa, Y.; Abe, H.; Fujita, M.; Iwata, T.; Inoue, Y.; Doi, Y. *Macromol. Chem. Phys.* **2003**, *204*, 1822−1831.

(17) Maillard, D.; Prud'homme, R. E. *Macromolecules* **2006**, *39*, 4272−4275.

(18) Maillard, D.; Prud'homme, R. E. *Macromolecules* **2008**, *41*, 1705−1712.

(19) Maillard, D.; Prud'homme, R. E. *Macromolecules* **2010**, *43*, 4006−4010.

(20) Tsuji, H.; Ikada, Y. *Macromolecules* **1993**, *26*, 6918−6926.

(21) Tsuji, H.; Hyon, S.-H.; Ikada, Y. *Macromolecules* **1991**, *24*, 5651−5656.

(22) Keith, H. D.; Padden, F. J., Jr. *Polymer* **1984**, *25*, 28−42.

(23) Keith, H. D.; Padden, F. J., Jr.; Lotz, B.; Wittmann, J. C. *Macromolecules* **1989**, *22*, 2230−2238.

(24) Keith, H. D. *Polymer* **2001**, *42*, 9987−9993.

(25) Lotz, B.; Cheng, S. Z. D. *Polymer* **2005**, *46*, 577−610.

(26) Ye, H.-M.; Wang, J.-S.; Tang, S.; Xu, J.; Feng, X.-Q.; Guo, B.-H.; Xie, X.-M.; Zhou, J.-J.; Li, L.; Wu, Q.; Chen, G.-Q. *Macromolecules* **2010**, *43*, 5762−5770.
(27) Rosenthal, M.; Portale, G.; Burghammer, M.; Bar, G.; Samulski, E. T.; Ivanov, D. A. *Macromolecules* **2012**, *45*, 7454−7460.
(28) Kawai, T.; Ehara, K.; Sasano, H.; Kamide, K. *Makromol. Chem.* **1968**, *111*, 271−276.
(29) Dorgan, J. R.; Williams, J. S.; Lewis, D. N. *J. Rheol.* **1999**, *43*, 1141−1155.
(30) Grijpma, D. W.; Penning, J. P.; Pennings, A. J. *Colloid Polym. Sci.* **1994**, *272*, 1068−1081.